

# Avances tecnológicos para vehículos inteligentes: control compartido en contextos de alta complejidad y automatización del transporte en entornos segregados

## Technological advances for intelligent vehicles: shared control in highly complex contexts and the automation of transport in segregated environments

Jorge Villagra<sup>1\*</sup>, Joan Vallvé<sup>2</sup>, Juan Medina-Lee<sup>1</sup>, Joan Solà<sup>2</sup>, Antonio Artuñedo<sup>1</sup>, Juan Andrade-Cetto<sup>2</sup>

<sup>1</sup> Centro de Automática y Robótica, CAR, CSIC-UPM, Ctra. Campo Real Km 0,2, 28500 Arganda del Rey, Madrid

<sup>2</sup> Institut de Robòtica i Informàtica Industrial, CSIC-UPC, c/Llorens i Artigas 4-6, 08028 Barcelona

\* Corresponding author: jorge.villagra@csic.es



### Abstract

To make autonomous driving a mass reality in cities there are still important technological barriers to be solved. It is therefore foreseeable that its implementation will be gradual, prioritising its appearance in operational environments of limited complexity, or taking into account that human intervention might eventually be required, in a paradigm of shared responsibility between the machine and the driver. The groups of Automated and Connected Driving at CAR, and Mobile Robotics at IRI, both from CSIC, propose in this article their contributions in these two complementary lines of research.

### Resumen

Para hacer que la conducción autónoma se convierta en una realidad de masas en las ciudades existen aún importantes barreras tecnológicas por resolver. Es previsible por tanto que su implantación sea gradual, priorizando su aparición en entornos operacionales de complejidad acotada, o requiriendo eventualmente la intervención humana en un paradigma de responsabilidad compartida entre la máquina y el conductor. Los grupos de Conducción Automatizada y Conectada del CAR y de Robótica Móvil del IRI, ambos del CSIC, proponen en este artículo sus contribuciones en esas dos líneas de actuación complementarias.

### 1. Introduction

Cities and metropolitan areas are the hubs of global growth, reaching over 80% of the world's population by 2050 [1]. This growing urbanization is generating unregulated growth, with inadequate and overloaded infrastructure and services, with the transport of goods and people being one of the clearest examples of inefficiency and negative impact on air pollution. In this connection, Goal 11 of UN SDG<sup>1</sup> has among its targets to provide access to safe, affordable, accessible, sustainable transport systems for all and to improve road safety, paying special attention to the

needs of people in vulnerable situations. To tackle this challenge, it is essential to rethink our large urban areas and orient them towards a zero-carbon future, and innovation in urban mobility has great potential to foster this necessary transformation.

Mobility as a service (MaaS) can be an effective tool to pursue these ambitious environmental objectives, moving users away from private cars while promoting a more carbon-efficient mobility mix. However, this new paradigm will only be able to respond to the challenges evoked by SDG 11 if the premises of inclusion and equity of access to this model are respected. The technology that can undoubtedly provide an answer to this challenge and decisively support the change of paradigm inspired by the MaaS is autonomous driving. In fact, if intelligently integrated with the different forms of public transport, shared autonomous vehicles can contribute decisively to improving the current negative aspects of urban mobility by making it more affordable, efficient, easy to use and available to all. However, in urban environments where complexity and unpredictability are huge, we are still far from being able to deploy safe solutions. This article presents two works in complementary application fields that aim to reduce the gap of current technological constraints: shared control in highly complex contexts and the automation of transport in segregated environments such as ports.

### 2. Shared autonomy

Different automation systems for the driving process have been introduced over the last years. Although these systems have significantly progressed, they still need the human driver intervention to handle all possible situations in a safely manner. Human-machine interaction has been addressed in some recent EU-funded research projects. The AutoMate project<sup>2</sup> focuses on driver-automation interaction and communication with other vehicles for SAE Level 3 and above. To that end, different levels of cooperation are introduced to achieve a successful human-machine interaction. In contrast, the Vi-DAS project<sup>3</sup>

<sup>1</sup> <https://www.un.org/sustainabledevelopment/>

<sup>2</sup> <http://www.automate-project.eu/>

<sup>3</sup> <http://vi-das.eu/>

focuses on the development of intuitive HMI to warn and assist the driver in anticipating potentially critical events by applying the latest advances in sensors, data fusion and machine learning. Moreover, The ADAS&ME project<sup>4</sup> addresses the transition between SAE0 - SAE3 automation levels, considering the driver state with regard to its attention, visual/cognitive distraction, stress, workload, emotions, sleepiness and fainting. These traded control strategies may lead to wrong behaviors if not implemented correctly, so it still remains a big challenge of assistive technologies in automobiles [2].

In this context, the PRYSTINE project [3] explores an alternative view where vehicles and humans may need to adapt their cooperation level depending on the context. To that end, it defines and assigns a Complexity Level (CL) to each driving scene in real time and defines the role of the Automated Driving System (ADS) and the human operator accordingly. The CL of the scene depends on the number and quality of the trajectory candidates generated by the ADS, which is significantly different when driving into a highly occupied roundabout than navigating on a highway at off-peak hours. When the CL decreases, the proposed ADS changes the level of driving automation accordingly, and can handle more driving tasks without human intervention. Nevertheless, the human operator must be prepared for an eventual system-to-human transition of control to avoid undesirable consequences [4]; for that reason, a Driving Monitoring System (DMS) needs to constantly estimate the involvement level of the human operator. With this information in hand the

ADS may generate a warning when the involvement of the human is lower than recommended, so the situation awareness is kept at safe levels.

The proposed architecture includes a robust decision-making system that correctly responds to difficult scenarios and trades control of the vehicle with the human pilot when necessary through the use of three main building blocks: a maneuvers planner, a trajectory generator and a supervision process.

**Maneuver Planner:** it narrows the possible navigable corridors for the ego-vehicle. It uses information about traffic, obstacles and global routing to decide which of the available corridors is/re the most pertinent for the trajectory generator. This hierarchical architecture allows the system to execute strategic maneuvers like overtake or change global route when a lane is blocked.

**Trajectory generator.** First, a set of trajectories are generated into the possible navigable lanes of the ego-vehicle. Each trajectory consists of a path created using a 5th order Bézier curve and a speed profile consistent with safety and comfort requirements. The complete process of the trajectory generation is described in [5]. Once a candidate is complete, some of its features like its acceleration, jerk or average speed data are stored as Trajectory Performance Indicators (TPI). These TPI are combined in a merit function in order to select the best possible candidate for a given driving style.

Figure 1 shows the trajectory generation process when the ego-vehicle is approaching a roundabout where two dynamic obstacles (vehicles) evolve.

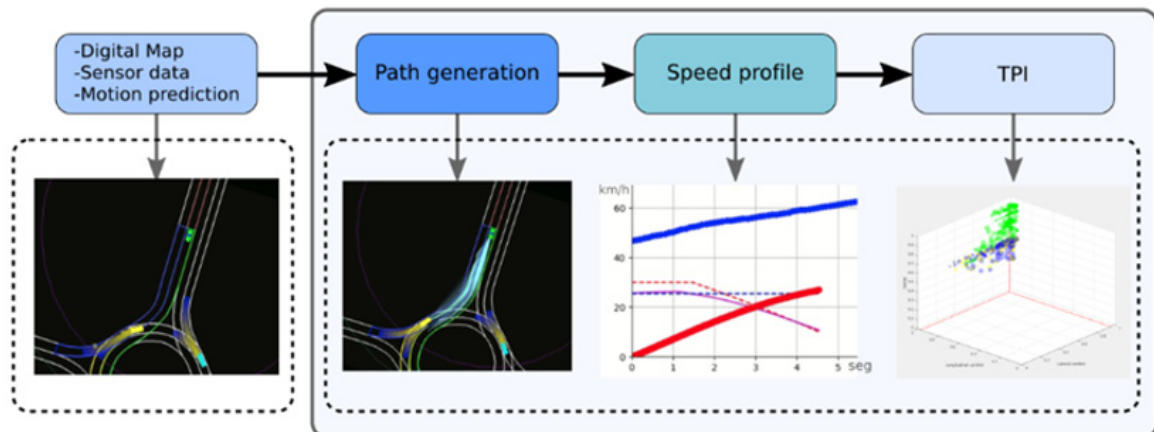


Figure 1. Trajectory generation process.

Figura 1. Proceso de generación de trayectorias.

The merit of each candidate is computed using four decision variables: longitudinal comfort, lateral comfort, safety and utility, each of which is computed using a set of TPIs, as showed in Figure 2. Longitudinal and lateral comfort are computed using the maximum and average values of the corresponding acceleration and jerk. The only difference is that the lateral comfort also takes into account the smoothness of the path. The safety variable depends on four TPIs. Free ride

and closeness TPIs describe how much the ego-vehicle approaches to static obstacles or dangerous zones; while safe chase indicates the safe distance to dynamic obstacles on the scene and lane invasion measures the maximum distance that a candidate occupies an adjacent lane. The Utility variable uses the average speed along the trajectory, the length of the path and the information of the obstacles present along the way.

<sup>4</sup> <http://www.adasandme.com/>

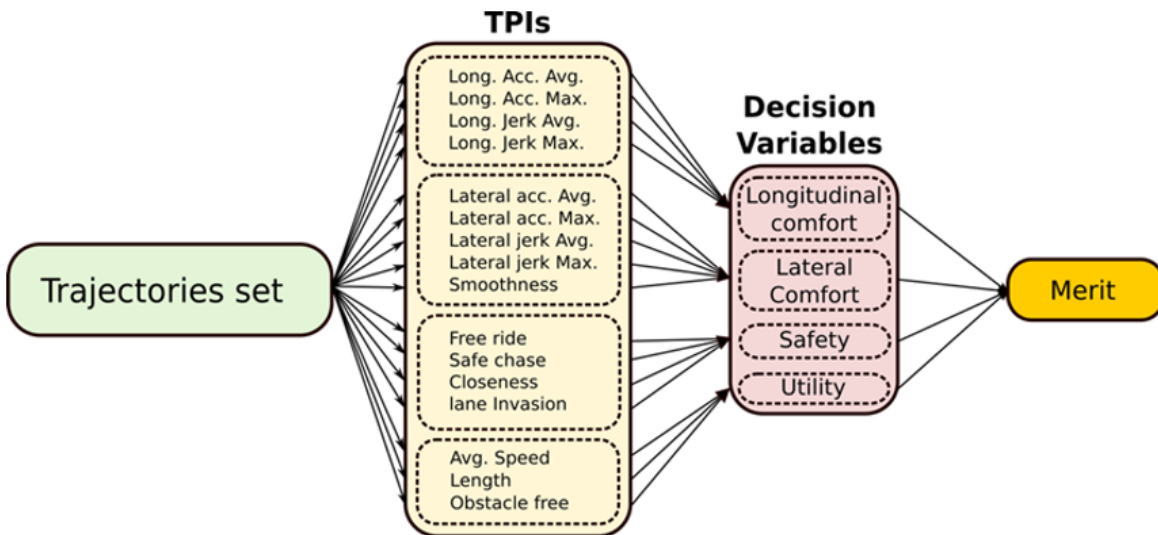


Figure 2. Trajectory performance indicators for merit computation.

Figura 2. Indicadores de rendimiento de la trayectoria para el cálculo de méritos.

**Supervisor:** It is in charge of three main tasks, as depicted in Figure 3. Firstly, it determines if it is necessary to update the current trajectory of the ego-vehicle and selects the trajectory candidate that maximizes the merit function. Then, the traded control task decides the CL of the scene in real time, and finally suggests the most appropriate

involvement level from the human driver accordingly. An HMI allows a complete interaction between the human and the ADS, showing to the human driver the proposed driving trajectory, the vehicle status or the recommended involvement level; the HMI also displays warnings and make trading control requests (including safe-stop maneuver) when necessary.

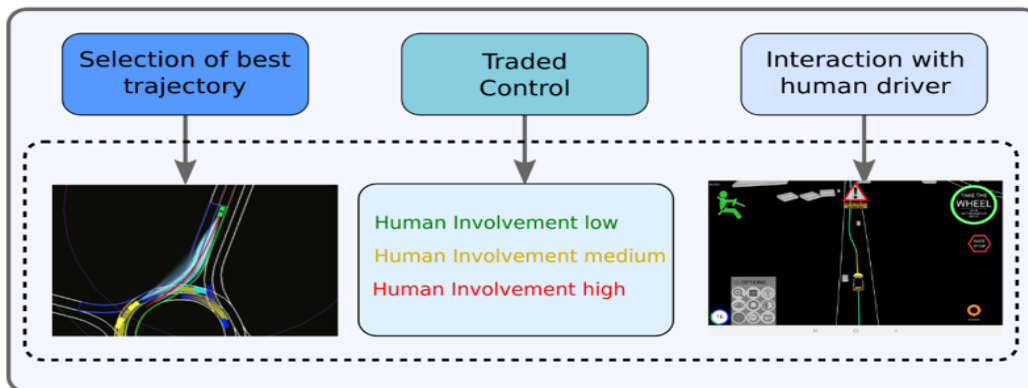


Figure 3. Supervisor module of the decision-making system.

Figura 3. Módulo de supervisión del sistema de toma de decisiones.

To evaluate the performance of the system, it was proposed a setup on a simulation environment where the autonomous vehicle had to face urban scenarios

like four-way intersections or roundabouts. Figure 4 shows the different scenes of the simulation setup.

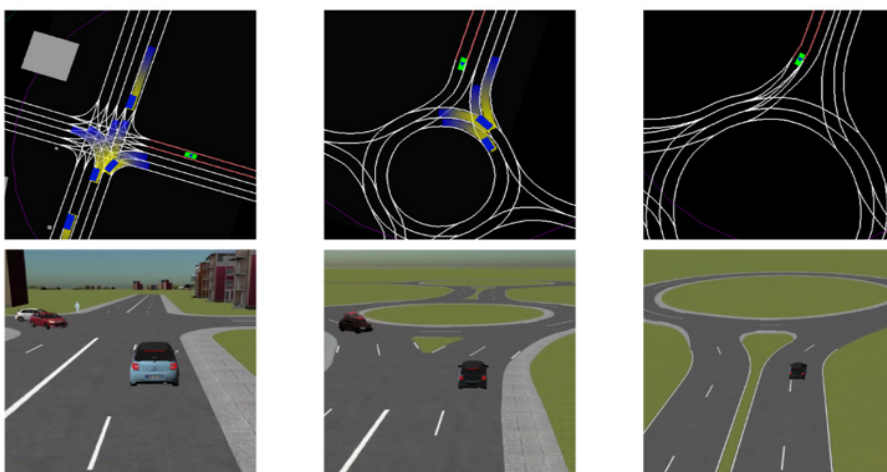


Figure 4. Setup on simulation environment. The first scene is a four-way intersection (a). The second scene is a roundabout with medium traffic (b) and at the end there is another roundabout with no traffic (c).

Figura 4. Configuración en un entorno de simulación. La primera escena es una intersección en X (a). La segunda escena es una rotonda con tráfico medio (b) y al final hay otra rotonda sin tráfico (c).

The experiment consisted of letting the autonomous system handle the three scenarios and then analyzing the final trajectory and the level of involvement required from the human driver along the way. Figure 5 shows the complete trajectory followed by the ego-

vehicle after the experiment. Red sections indicate complex scenes where the involvement from the human driver needed to be high, and green sections required low involvement from the human driver.

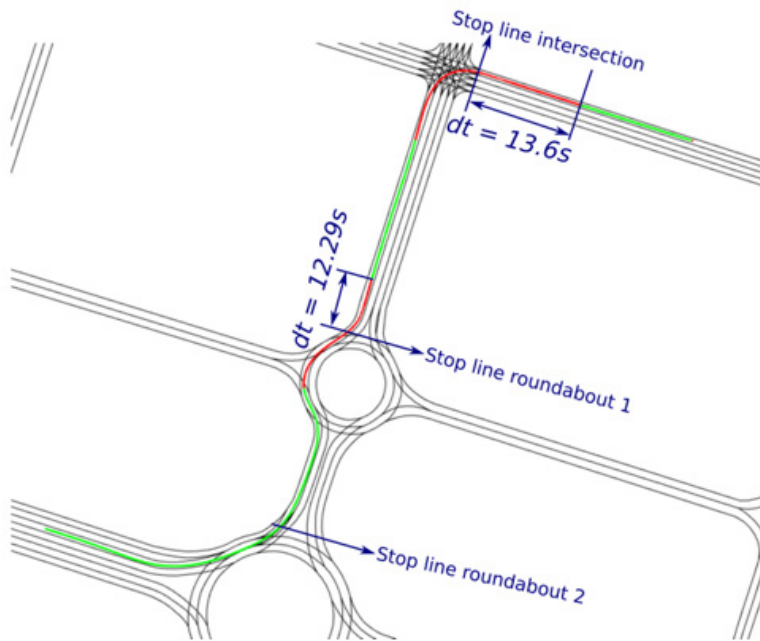


Figure 5. Complete trajectory followed by the autonomous vehicle.

Figura 5. Trayectoria completa seguida por el vehículo autónomo.

In the case of the four-way intersection, the complex scene was detected (and therefore a high involvement required from the driver) with a time in advance of 13.6s before the stop line is reached; in the case of the roundabout, this lead time was 12.29s. These intervals provide the driver time enough to safely regain control as, according to the literature [6], the estimated time for average humans to take-over is

between 6s and 10s. These satisfactory results were confirmed on a real driving scenario with one of the AUTOPIA<sup>5</sup> automated vehicles, as shown in Figure 6. In these experiments, the HMI and the DMS, developed by our partner ROVIMATICA, are shown when a safe-stop is conducted by the ADS due to the driver drowsy state (image on the right bottom corner and red icon on the right upper part of the figure).

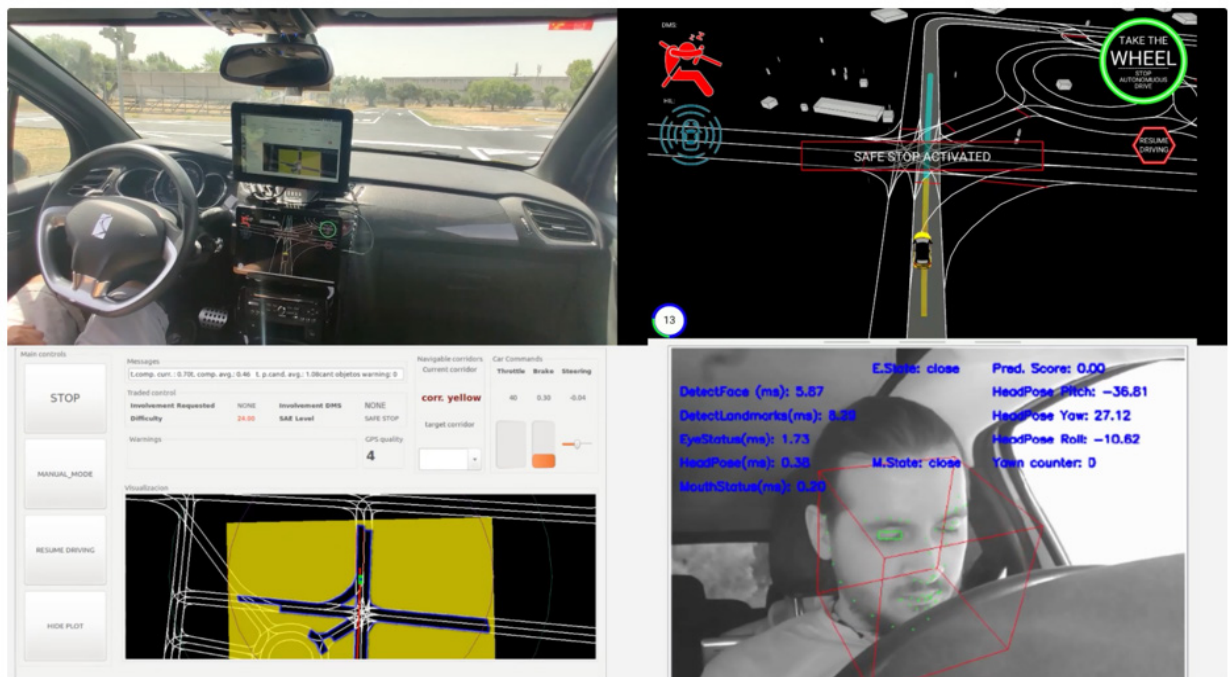


Figure 6. Traded control on a real experiment: (a) inside of the vehicle; (b) HMI; (c) development interface; (d) DMS.

Figura 6. Cambio de control en un experimento real: (a) dentro del vehículo; (b) HMI; (c) interfaz de desarrollo; (d) DMS.

<sup>5</sup> <https://autopia.car.upm-csic.es>

### 3. Autonomous transportation of freight in small cargo container terminals

Currently, the expected increase in the annual volume of port logistics vehicles between 2018 and 2023 is estimated at 3.8%. This significant increase in port activity, together with the scarcity of adjacent land that prevents them from expanding their infrastructures, means that there is need for more efficient and profitable means for the use of port vehicles, which allow improving the management of port logistics in conditions of high congestion and capacity.

Optimization of operations in harbor -and inland-container terminals is mainly limited by non-negligible and unforeseen manually driven maneuvers. Despite progress in autonomous vehicles, their benefits have not widespread to the container handling operations due to various reasons, such as different shipping modalities of several terminals and safety related restrictions (fencing). Moreover, the implementation of automated systems often requires a substantial investment to equip the terminal ground with a grid of transponders allowing full localization and control of the automated guided vehicles. This large economic investment is preventing smaller terminals to adopt automation solutions.

The Cargo-ANTs project<sup>6</sup> developed innovative solution for vehicle automation in container terminals, focusing on automating maneuvers on a grid-less infrastructure, significantly lowering the investment requirements and hence extending the highly automated and yet extremely flexible flow of individual units of freight from- and to- cargo ships in harbor terminals and within inland terminals, thus specifically aimed to smaller terminals. This goal was achieved by adopting autonomous robotics research to develop a novel technology in the following innovation fields: full vehicle perception and dynamic- and static- object detection, local- and global- mapping, and autonomous path generation and following. The final demonstration of the project results was carried out in Stora Holm Traffic Training facilities near Gothenburg, Sweden, in August 2016.

The LOGIMATIC project<sup>7</sup> developed an advanced autonomous location and navigation solution based on EGNSS satellite positioning systems (GALILEO) and on sensors on board straddle carriers (forklift and bridge crane assembly that allow moving containers). A GIS control module was also implemented compatible with the current terminal operation systems for the global optimization of routes and management of the SC vehicle fleet, as well as a system to detect and prevent possible computer sabotage navigation systems. The results of the project were successfully tested in the port of Thessaloniki, Greece, in August 2019.

Summarized results are reported here on the topics of radar-based odometry estimation, localization and mapping for the Cargo-ANTs project, and on EGNSS-based localization and mapping for the Logimatic project.

#### Radar-based odometry estimation

Accurate vehicle localization of autonomous vehicles is usually estimated by fusing data from multiple sources, odometry being one of them. Large vehicles such as straddle carriers often do not have accurate odometry units, and odometry estimates need be computed from alternative sensors. In Cargo-ANTs, an innovative approach for the computation of odometry estimates from stereo radar signals was developed [7]. The approach is based on the Doppler velocity received by a pair of automotive radars mounted on the vehicle. The study was aimed at computing the optimal mounting point of these two sensors in the vehicle, in order to minimize the final uncertainty of the estimated vehicle twist (rotational and linear velocities), which is computed from the radar azimuth and the Doppler data. Figure 7 shows the results on an experimental research platform. The conclusion being that optimal sensor placement is at opposite ends of the vehicle frame. The obtained vehicle odometry estimate was used as an extra constraint for both localization in a previously built map, and full simultaneous localization and mapping.

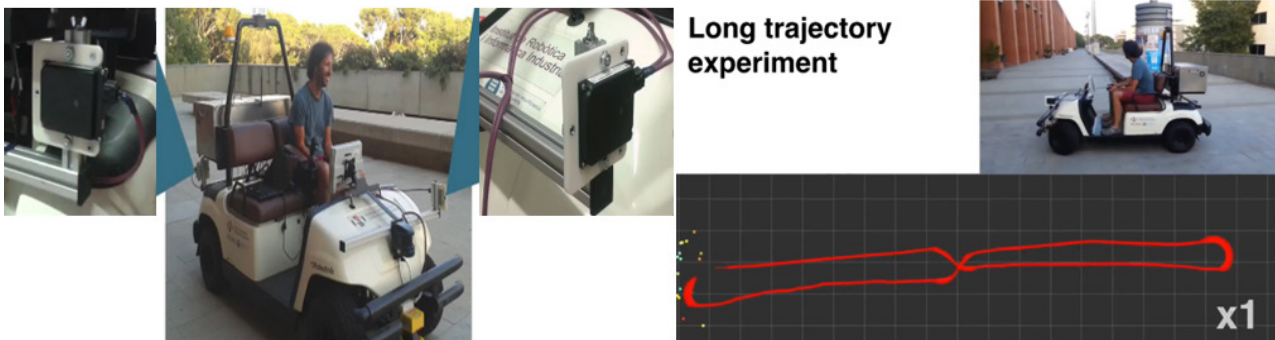


Figure 7. Stereo radar odometry setup in an experimental robotics platform.

Figura 7. Configuración de odometría de radar estéreo en una plataforma de robótica experimental.

<sup>6</sup> <https://www.iri.upc.edu/project/show/133>

<sup>7</sup> <https://logimatic-project.eu>

### Localization and mapping

In a cargo container terminal, the environment is highly structured, with buildings and containers representing large features to which a vehicle can localize with large precision at the centimeter level, even in situations with denied or weak GNSS positioning estimates. This is particularly important for tasks such as container loading and unloading. The localization and mapping tasks were addressed by solving a geometric constrained optimization where the free parameters were all the poses of the vehicle trajectory as well as the absolute positioning of naturally identified landmarks [8]. The considered landmarks consisted of extracted polylines,

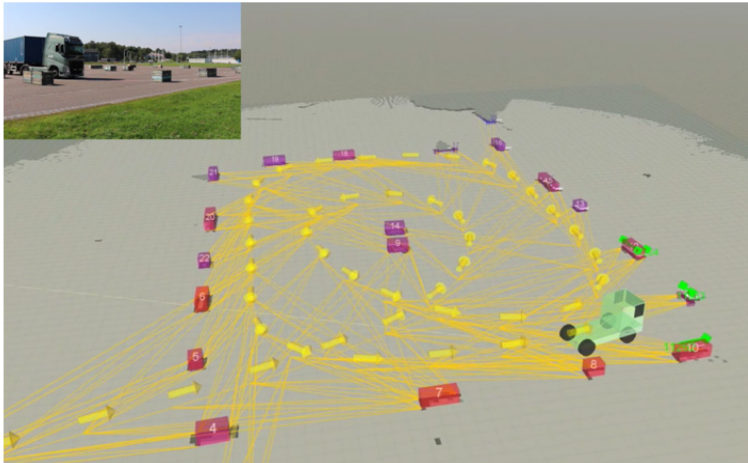


**Figure 8.** Simultaneous Localization and Mapping (SLAM) session during the final demonstration event.

**Figura 8.** Sesión de Localización y Cartografía Simultáneas (SLAM) durante el evento final de demostración.

### Multi-sensor integration for local positioning and navigation

The main objective was to develop a self-contained localization module that relies only on on-board sensors, but that is conceived as an open architecture to be integrated with absolute measurements coming from the GNSS/EGNOS localization unit.

The work performed included the development of a localization and mapping solution using primarily lidar sensing as well as odometry from a straddle carrier. As with the case of the automated truck, the method developed consisted on the optimization of a large network of geometric constraints. The large networks produced called for research on methods to sparsify these networks of geometric constraints to make computation tractable. The chosen solution was obtained by minimizing the

divergence of the resulting network compared to the original one [9]. Secondly, a method for the detection of loop closures purely from the signature of the lidar readouts was also developed [10] the map is encoded as a graph of poses, and to cope with very large mapping capabilities, loop closures are asserted by comparing the features extracted from a query laser scan against a previously acquired corpus of scan features using a bag-of-words (BoW). A general programming framework was developed that integrates the optimization problem, together with these two contributions. The framework was named WOLF for (window of localization frames). Simulations results in a port setting with the kinematic model of a straddle carrier are shown in Figure 9. The next step is to include in this framework the tight integration of our GNSS solution.

divergence of the resulting network compared to the original one [9]. Secondly, a method for the detection of loop closures purely from the signature of the lidar readouts was also developed [10] the map is encoded as a graph of poses, and to cope with very large mapping capabilities, loop closures are asserted by comparing the features extracted from a query laser scan against a previously acquired corpus of scan features using a bag-of-words (BoW). A general programming framework was developed that integrates the optimization problem, together with these two contributions. The framework was named WOLF for (window of localization frames). Simulations results in a port setting with the kinematic model of a straddle carrier are shown in Figure 9. The next step is to include in this framework the tight integration of our GNSS solution.

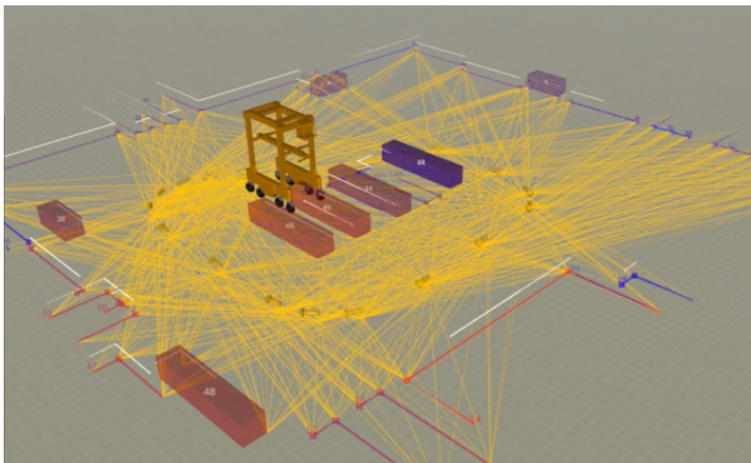


**Figure 9.** Simulation results of local position estimation from onboard sensors for a straddle carrier.

**Figura 9.** Resultados de la simulación de la estimación de la posición local a partir de los sensores a bordo para una grúa de carga a horcajadas.

### Integration of multi-constellation GNSS/EGNOS signals and self-localization multi-sensor based techniques

An EGNOS-augmented standalone GNSS fix provides the required sub-meter accuracy for vehicle localization and navigation. In Logimatic, a different approach was investigated. Localization and mapping is provided by local sensing and GNSS is used only to compute precise motion estimation between any two points in the trajectory, which is fed to the local mapping algorithm. The origin and destination of this computation is triggered by the SLAM framework so there is no predefined frequency, period or distance even though this influences the performance. A GNSS standalone solution is of course provided by all commercial receivers off-the-shelf. Logimatic proposes to extend this by computing the single differences of pseudo-ranges (SD) in order to obtain the displacement between two points with enhanced precision.

The most commonly used algorithm for position computations from pseudoranges is based on the iterative least-squares method (ILS). The geometrical constraints behind the ILS approach are equivalent to those exploited in the SD technique. SD computes in one LS iteration only the displacement between two different positions. ILS instead computes several iterations of the LS in SD between our current real position and an "approximated position". GNSS data from our current position is measured directly from the receiver. GNSS data from the guessed or virtual position is computed synthetically. The displacement between our real position and the approximate position can be understood as an error or correction to be applied iteratively until the approximation converges. This method for our experience converges

in 4 or 5 iterations. This is reduced to 1 or 2 if we use the previous position as a prior.

Figure 10 shows the accuracy of the proposed solution versus the proprietary solution of the receiver manufacturer. The figure shows position errors fusing receiver fixes and odometry, fusing the latter two with single-differences displacement vectors, and fusing the latter three with onboard lidar. The objective is to qualitatively illustrate the distribution and location of the error along the trajectory. The retrofitted SC has a series of kinematic parameters difficult to measure and calibrate, and as such, provide inaccurate odometric translation measures. This is alleviated by the use of the SD and the GNSS fixes, but at some point is not sufficient. However, solutions based only on GNSS fix (i.e. Septentrio proprietary and SLAM odom+fix) concentrate the errors in different areas than the ones incorporating single difference measurements. While the first ones are located at the surroundings of the cranes area, the SLAM solutions using SD measurements get some error peaks in open space. This is probably caused by misalignment of laser readings when there is no structure to link the laser to. On the other hand, the fusion of two different odometry estimates becomes more valuable in regions with GNSS blockage or multipath signal returns. Figure 11 shows a full session of localization and mapping overlaid on an aerial photograph of the Thessaloniki port. The blue and magenta axes indicate the EN and local reference frames, respectively. White areas indicate open space as registered by one of the LiDAR sensor onboard the vehicle.

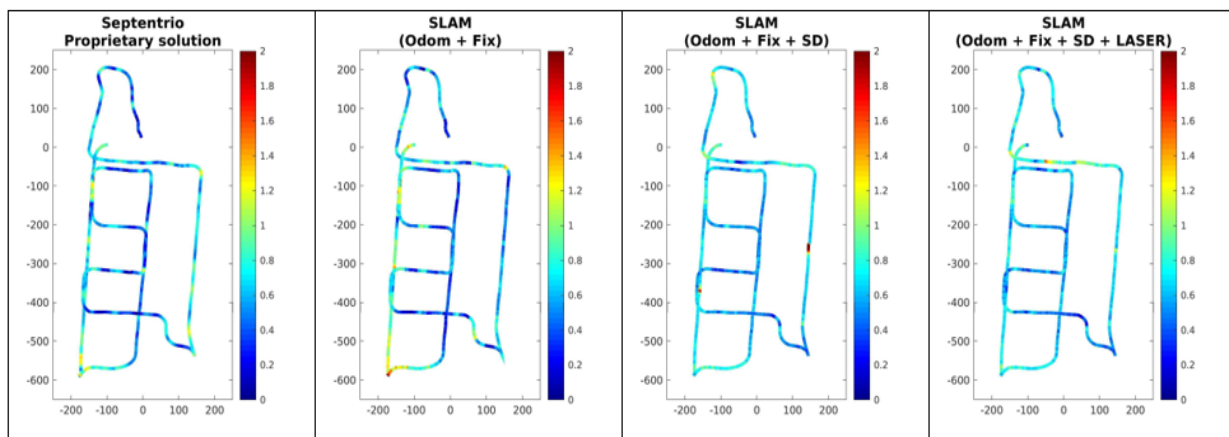


**Figure 10.** Position errors at several instants of the trajectory. Left: proprietary fix without odometry. Next: Fix and odometry. Second to right: SD displacement vectors, fix and odometry. Right: Laser, SD displacement vectors, fix and odometry. (Position errors in meters are color-coded).

**Figura 10.** Errores de posición en varios instantes de la trayectoria. A la izquierda: fijación propietaria sin odometría. Siguiente: Fijación y odometría. Segundo a la derecha: Vectores de desplazamiento SD, fijo y odometría. A la derecha: Láser, vectores de desplazamiento SD, fijo y odometría. (Los errores de posición en los medidores están codificados por colores).



**Figure 11.** The map is overlaid onto a georeferenced image using the optimized EN-to-SLAM frame transformation  $(X,Y,\theta)=(4.01m, 3.42m, 3.177rad)$  with an EN origin at  $(lat,lon)=(40.638972,22.907978)$ . Notice that the image and the map correspond to different days and hence some of the mapped features do not match.

**Figura 11.** El mapa se superpone a una imagen georreferenciada utilizando la transformación de cuadro EN a SLAM optimizada  $(X,Y,\theta)=(4,01m, 3,42m, 3,177rad)$  con un origen EN a  $(lat,lon)=(40.638972,22.907978)$ . Note que la imagen y el mapa corresponden a días diferentes y por lo tanto algunos de los rasgos mapeados no coinciden.

### 3. Conclusions

Although autonomous vehicles may become a norm in the future, we can safely assume that mixed traffic (non-, semi- and fully autonomous vehicles) is expected to be the reality for at least the next couple of decades. The cooperation between vehicles and with the infrastructure will be exploited in order to improve the safety of each vehicle, and in specific cases of complex resolution, with the aim of disbanding situations that today are unsolvable for an artificial decision system.

In a shorter period of time, it is foreseeable to see an increment of either solutions relying on a shared human-machine decision making paradigm, or full vehicle automation in segregated scenarios, such as the cargo scenario described in this paper, prior to the adoption of fully autonomous vehicles in mixed traffic. The reasons being not only the earlier technological feasibility, but also the ease of social acceptance due to the lower risk for humans, as well as the targeted economic impact that will drive a small number of companies to adopt these solutions.

### 4. Acknowledgements

Research groups Autopia (CAR) and Mobile Robotics (IRI).

PTI Mobility 2030 (<https://pti-mobility2030.csic.es/>)

### 5. References

- [1] European Commission, "The European Green Deal," in *European Commission*, 2019.
- [2] T. Inagaki and T. B. Sheridan, "A critique of the SAE conditional driving automation definition, and analyses of

options for improvement," *Cogn. Technol. Work*, vol. 21, no. 4, pp. 569–578, Nov. 2019.

[3] N. Druml *et al.*, "Programmable Systems for Intelligence in Automobiles (PRYSTINE): Technical Progress after Year 2," in *23rd Euromicro Conference on Digital System Design*, 2020, pp. 360–369.

[4] F. Biondi, I. Alvarez, and K.-A. Jeong, "Human-Vehicle Cooperation in Automated Driving: A Multidisciplinary Review and Appraisal," *Int. J. Human-Computer Interact.*, vol. 35, no. 11, pp. 932–946, Jul. 2019.

[5] A. Artunedo, J. Villagra, and J. Godoy, "Real-Time Motion Planning Approach for Automated Driving in Urban Environments," *IEEE Access*, vol. 7, pp. 180039–180053, 2019.

[6] F. Naujoks and A. Neukum, "Specificity and timing of advisory warnings based on cooperative perception," in *Mensch & Computer 2014 - Workshopband*, München: OLDENBOURG WISSENSCHAFTSVERLAG, 2014, pp. 229–238.

[7] A. Corominas-Murtra, J. Vallve, J. Sola, I. Flores, and J. Andrade-Cetto, "Observability analysis and optimal sensor placement in stereo radar odometry," in *Proceedings - IEEE International Conference on Robotics and Automation*, 2016, vol. 2016-June, pp. 3161–3166.

[8] J. Vallvé and J. Andrade-Cetto, "Active pose SLAM with RRT," in *Proceedings - IEEE International Conference on Robotics and Automation*, 2015, vol. 2015-June, no. June, pp. 2167–2173.

[9] J. Vallvé, J. Solà, and J. Andrade-Cetto, "Pose-graph SLAM sparsification using factor descent," *Rob. Auton. Syst.*, vol. 119, pp. 108–118, 2019.

[10] J. Deray, J. Sola, and J. Andrade-Cetto, "Word Ordering and Document Adjacency for Large Loop Closure Detection in 2-D Laser Maps," *IEEE Robot. Autom. Lett.*, vol. 2, no. 3, pp. 1532–1539, 2017.